Low-Temperature-Programmed Replacement of Nitrogen by Hydrogen in Pores of Mordenite

Shanmugam Yuvaraj,[†] Tsong-Huei Chang,[‡] and Chuin-Tih Yeh*[,†]

Department of Chemistry, National Tsing Hua University, Hsinchu 30043, Taiwan, ROC, and Department of Chemical Engineering, Ming Hsing University of Science and Technology, Hsinchu 30043, Taiwan, ROC

Received: July 22, 2002; In Final Form: March 24, 2003

Nitrogen molecules were filled in pores of NaMOR by calcination at $T_c = 773$ K under nitrogen atmosphere and then replaced by hydrogen molecules. The replacement was performed in a specially designed low-temperature routine operated between 173 and 423 K with a flow of 10% hydrogen in nitrogen. The obtained replacement profile comprised four kinds of phenomena, i.e., rapid replacement (R_r) of gaseous phase nitrogen in pores by hydrogen, hindered replacement (R_h) of nitrogen condensed around sodium ions, activated chemisorption of (C) of nitrogen molecules on sodium ions, and desorption (D) of chemisorbed nitrogen from Na^+ site. The R_r exhibited two major peaks at ∼185 and ∼240 K for nitrogen in 12-MR channel (R_{rc}) and in 8-MR side pocket (R_{rp}). The R_h was delayed up to 350 K due to hindrance by sodium ions. Both the C and the D exhibited three sharp peaks for sodium ions at three kinds of environments in MOR structure.

1. Introduction

Zeolites are inorganic microporous materials comprising a channel, cage, and pocket of various dimensions. The micropores in zeolites are embedded with nonframework cations (countercations) to maintain the charge neutrality of the framework. Many factors affect the diffusivity of gases through a zeolite. Noticeably, the dimension of pores, size of cations and diffusion molecules, and interaction of diffusing gases with cations are playing important role.[1] The variation in diffusivity of different gases in a mixture results in their separation into individual components.[2]

Mordenite (MOR) is a type of zeolite with pores of large channels and medium side pockets. Figure 1 describes the structure of the mordenite (MOR), whose channels (*z*-axis, 0.65 × 0.70 nm) are built by 12-membered ring (MR) windows. These channels are interconnected with side pockets of 0.48 nm deep (in *y*-axis) through an 8-MR opening (0.26 × 0.57 nm). The diffusion of gases in the pores should be significantly affected by the countercations. Three different locations (see Figure 1), i.e., A at the vicinity of 6-MR in channel, B at the intersection of the 8-MR connecting the side pocket to channel, and C in the side pocket, have been theoretically predicted for sodium in NaMOR (NaM).[3,4] Conceivably, the diffusion of molecular hydrogen ($d_{H_2} \sim 0.30$ nm) and nitrogen ($d_{N_2} \sim 0.4$ nm) into side pockets may be seriously hindered if the Na^+ ion ($d \sim 0.2$ nm) is at the intersection. Even in channels, the charge balancing sodium ions in NaM should pose an obstruction to traversing molecules.

It is expected that the channel, side pocket, and counterions in MOR should influence the diffusion of gases to different extents. The extent of influence can be monitored in terms of temperature required for the diffusion in a temperature-programmed profile. For this purpose, replacement of nitrogen molecules by hydrogen molecules in micropores of MOR is probed in a flow system employing a low-temperature routine (LTR). The LTR setup has been recently designed to characterize the redox phenomena of nanosized metals.[5]

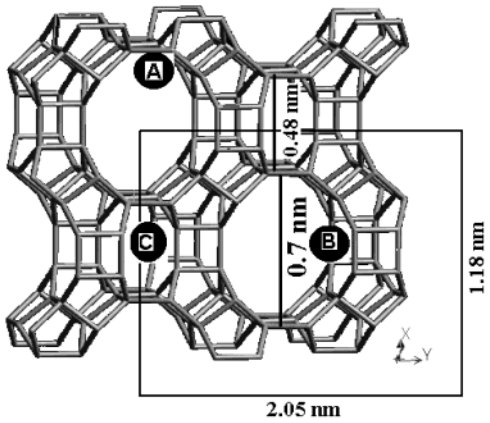

Figure 1. Model figure for NaM showing various locations (A−C) for sodium cations.

2. Experimental Section

2.1. Preparation of Samples. Zeolite KL (Si/Al = 3.4, K/Al ∼ 1.5 and surface area = 310 $m^2 \cdot g^{-1}$) was synthesized by a well-documented procedure.[6] Its protonic form (HL) was obtained through a calcination of ammonium ion-exchanged KL sample. NaMOR (Si/Al = 10; $N_{Na} = 4.8 \times 10^{20}$ atoms$\cdot g^{-1}$ and surface area = 340 $m^2 \cdot g^{-1}$) and HMOR (Si/Al ∼ 10; $N_{Na} = 2.9 \times 10^{18}$ atoms$\cdot g^{-1}$ and surface area = 380 $m^2 \cdot g^{-1}$) samples were obtained from Tosoh Corp.. The metal content of prepared samples was analyzed by ICP-AES analysis.

2.2. Replacement Reaction in a Low-Temperature Routine (LTR). About 100 mg of a sample was inserted in a U-shaped cell and precalcined (773 K) in nitrogen (special grade, 99.99%) flow. The sample was then cooled to 143 K, and then, the flowing stream was shifted to 10% H_2 in N_2. After a decent baseline was found from a thermal conductivity detector (TCD),

* Corresponding author. E-mail: ctyeh@mx.nthu.edu.tw.
† National Tsing Hua University.
‡ Ming Hsing Institute of Technology.

10.1021/jp026585w CCC: $25.00
Published on Web 05/02/2003

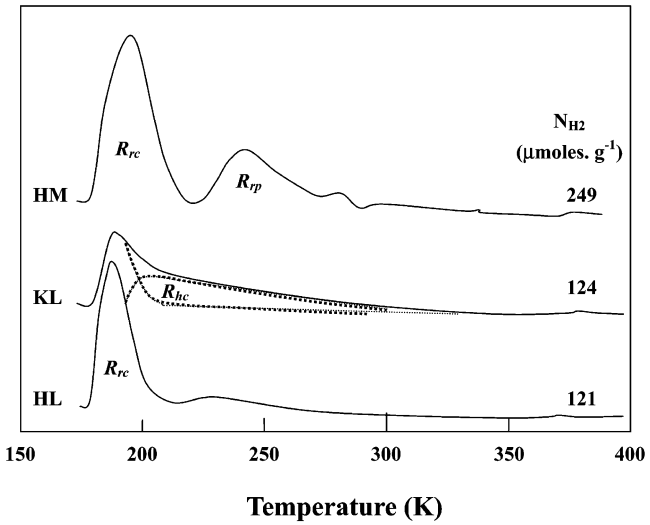

Figure 2. Low-temperature nitrogen replacement profiles of HL, KL, and HM samples.

replacement of nitrogen by hydrogen was recorded by the TCD on raising the system temperature from 173 to 423 K at a rate of 5 K·min^{-1}. Under the flow of 10% H_2 in N_2, positive peaks in a profile refer to nitrogen desorption and negative peaks are ascribed for uptake of nitrogen. In quantification, area of replacement peaks in temperature profiles is calibrated using 100% hydrogen. However, the minor peaks are quantified on the basis of 100% nitrogen assuming that these peaks result from nitrogen.

3. Results and Discussion

Figure 2 compares the replacement profiles of HL, KL, and HM zeolites. The profiles of HL and KL samples are presented on purpose to understand the effects of channel and cation on the replacement reaction. It is also pointed out that the channel dimension (0.7 × 0.7 nm)[7] in zeolite KL and HL is one-dimensional and rather similar to that of HM (and, of course, NaM too). A symmetrical peak centered at ∼185 K is noticed as the major signal in the profile of HL. Because the channels in HL are uniform columns,[7] the peak (N_{H_2} ∼ 101 μmol·g^{-1}) must result from a rapid replacement (R_{rc}) of gas-phase nitrogen molecules in the channels by hydrogen molecules. A minor and broad peak (N_{H_2} ∼ 20 μmol·g^{-1}) is barely noticed around ∼230 K in the profile and assigned to replacement of free nitrogen trapped in channel defects.

Profile KL also showed a low-temperature peak at 185 K, but it is trailed up to 350 K. The trailed peak may be deconvoluted into two peaks, viz., a sharp peak at 185 K and a broad peak in a high-temperature range of 220−330 K. The sharp peak in the KL profile is consistent with the R_{rc} of the HL profile and is also assigned for R_{rc} in the KL channel. Because the structures of KL and HL samples are the same but differ only with the cation, the trailed broad peak found in the profile of KL must be due to big K^+ ions protruding in the channel and is assigned to the hindered replacement (R_{hc}) of nitrogen in channel.

Table 1 lists the quantified amount of hydrogen involved in nitrogen replacement in peaks of R_{rc} and R_{hc} shown in Figure 2. The combined amount (∼124 μmol·g^{-1}) of R_{rc} and R_{hc} in the KL sample moderately exceeds the value of R_{rc} (N_{H_2} ∼ 101 μmol·g^{-1}) of HL sample. The excess suggests an accumulation of nitrogen molecules around potassium ions to form a condensed nitrogen sphere in the channels below 180 K.

TABLE 1: Assignments of Peaks Observed in Low-Temperature Nitrogen Replacement in Pores of L and MOR Zeolites

zeolite	peak notation	peak temp (K)	N_{H_2} (μmol·g^{-1})	$10^{-2}N_{N_2}/N_{Na}$	location
HL	R_{rc}	185	101		channel
KL	R_{rc}	185	67		channel
	R_{hc}	220	57		channel
HM	R_{rc}	185	165		channel
	R_{rp}	240	84		pocket
NaM	R_{rc}	185	95		channel
	R_{hc}	220	65		channel
	R_{rp}	240	60		pocket
	R_{hp}	250−330	115		pocket
	C_1	273	34[a]	4.3	channel
	C_2	283	60[a]	7.5	channel
	C_3	340	34[a]	4.3	channel
	D_1	300	34[a]	4.3	channel
	D_2	350	51[a]	6.4	channel
	D_3	390	76[a]	9.5	channel

[a] $a = N_{N_2}$ (μmol·g^{-1}).

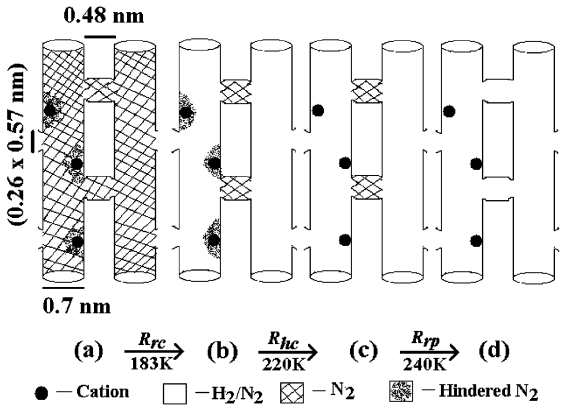

Figure 3. Model figure showing the nitrogen replacements by hydrogen in the channel and side pocket of K(HM).

Conceivably, the obvious delay of R_{hc} to a high temperature (220−350 K) results from an interaction of the condensed nitrogen with potassium ions.

Two symmetrical peaks (∼185 and ∼240 K) were clearly seen in the profile of HM. The peak at ∼185 K (N_{H_2} ∼ 165 μmol·g^{-1}) is retained to R_{rc} for rapid replacement of nitrogen in the channels of MOR. From the structural difference between L and MOR, the peak at 240 K must result from a rapid replacement of gaseous nitrogen in the side pockets (R_{rp}, 84 μmol g^{-1}) of HM.

All the peaks in Figure 2 may be explained through a convenient fictitious MOR model with potassium ions in the channels, as shown in Figure 3. It is remember that potassium ions are not really exchanged in the channels of MOR but incorporated in the model only to show the cation effect in the channels of KL. Figure 3a describes a MOR zeolite with potassium ions (depicted as small closed circles) only in channels (depicted as vertical columns, which also resemble the channels in KL) of MOR structure. After calcination, nitrogen molecules are filled (shown as cross-lines) in the columns and the side tubes, and condensed (depicted as dotted portion) around potassium ions. On increasing the sample temperature to 185 K, the nitrogen molecules in the channels are rapidly replaced (Figure 3b, R_{rc}) by H_2. However, the hindered replacement of condensed nitrogen molecules in channels (Figure 3c, R_{hc}) takes place at a high temperature, ∼220 K. The rapid replacement of nitrogen in the side pockets (Figure 3d, R_{rp}) by hydrogen occurs at 240 K.

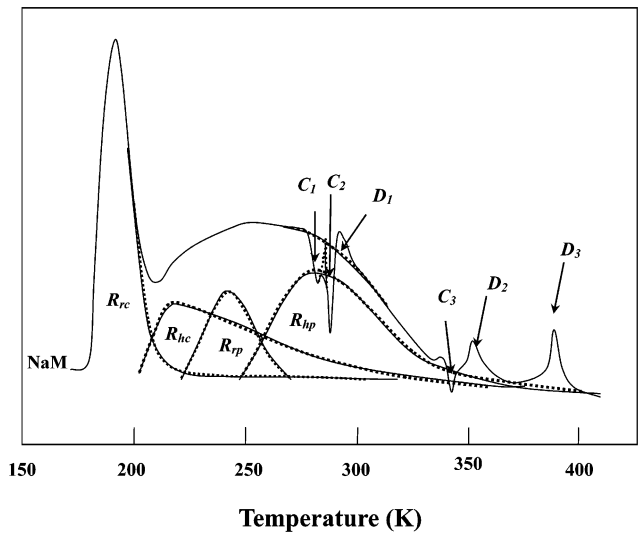

Figure 4. Low-temperature nitrogen replacement profile of NaM sample.

A complicated profile (Figure 4) was experimentally obtained from nitrogen replacement of NaM sample. Besides a broad trailed peak between 173 and 350 K, several minor features are also observed. A deconvolution of the broad peak led to four major peaks at ∼185, 220, 240, and 270 K. According to the previous assignments for similar peaks in KL and HM samples, peaks at ∼185, 220, and 240 K are ascribed to R_{rc} ($N_{H_2} \sim 95\ \mu mol \cdot g^{-1}$), R_{hc} ($N_{H_2} \sim 65\ \mu mol \cdot g^{-1}$), and R_{rp} ($N_{H_2} \sim 60\ \mu mol \cdot g^{-1}$) in the NaM crystallites.

A huge deconvoluted peak ($N_{H_2} \sim 115\ \mu mol \cdot g^{-1}$) is also seen around 270 K and may be ascribed to a hindered replacement of nitrogen in the side pockets (R_{hp}). The size of R_{hp} is almost twice that of R_{rp} of HM. The difference ($N_{H_2} \sim 55\ \mu mol \cdot g^{-1}$) in peak size revealed a prominent role of sodium cation toward condensing the nitrogen into the side pockets. Understandably, the replacement of these condensed-nitrogen molecules around sodium ions in side pockets extends to the high-temperature range (250−350 K).

Apart from replacement peaks, six minor sharp peaks are noticed in the profile of NaM. Among them, three are negative peaks, viz., C_1, C_2, and C_3, and the rest are positive peaks, viz., D_1, D_2, and D_3. In the present TPR study, negative and positive peaks can be ascribed to uptake and desorption of nitrogen, respectively. In the literature, the binding of atomic nitrogen to the silica framework in defect sites in the MOR structure has been reported at high temperature (673 K).[8] However, in this study, desorption of chemisorbed nitrogen is observed at a much lower temperature (<400 K), which indicates that nitrogen may be chemisorbed associatively rather than dissociatively:

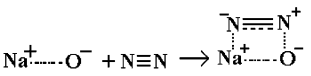

The three sharp negative peaks (C_1, C_2, and C_3) observed in the NaM profile are therefore assigned to activated chemisorption of nitrogen on sodium−oxygen ionic pair. A ratio ($N_{N_2}/N_{Na} \sim 0.16$) of the sum of nitrogen chemisorbed in these three peaks ($C_1 + C_2 + C_3$, Table 1) to the amount of sodium ions clearly indicates that only ∼16% of total sodium ions chemisorb nitrogen molecules.

Three sharp positive peaks (D_1, D_2, and D_3) seen in Figure 4 in respective temperatures at 300, 350, and 390 K. Arguably, on increasing the system temperature, thermal forces overcome the binding energy of chemisorbed nitrogen molecule and, thus, get desorbed from sodium ions:

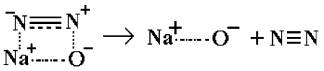

Therefore, these peaks are ascribed for desorption of chemisorbed nitrogen and Table 1 presents quantified data on these three peaks.

From Table 1, a ratio ($N_{N_2}/N_{Na} \sim 0.20$) of the amount of nitrogen desorbed ($D_1 + D_2 + D_3$) to the amount of sodium ions revealed that only ∼20% of total sodium ions chemisorbed nitrogen. The amount (16%) of sodium ions involved in chemisorption is comparable to that (∼20%) involved in desorption of chemisorbed nitrogen. The similar ratios suggested that desorption and chemisorption of nitrogen may have occurred on the same sodium ions.

The N_{N_2}/N_{Na} ratio (0.18 ± 0.02) is quantitatively determined for nitrogen chemisorbed in C peaks and desorbed in D peaks. According to the literature,[9] sodium ions are mainly located at three different locations in the MOR structure, i.e., in channels, at the intersection, and in side pockets, illustrated as A, B, and C in Figure 1. Many researchers have reported a population ratio of sodium ions in these three sites.[9−13] From the literature reports,[9−13] an average population ratio of sodium ions in locations at A, B, and C sites are approximately 16, 34, and 50%, respectively. The N_{N_2}/N_{Na} ratio is close to the ratio of sodium ions at site A, and the agreement suggests that only those sodium ions at site A might uptake nitrogen in a chemisorptive manner. Further, in view of the diffusional constraint at the intersection, broad and diffuse peaks are expected for nitrogen uptake/desorption from sodium ions in sites B and C. Hence, the three observed sharp peaks probably resulted from sodium ions in an A location (channel).

Further, sodium in site A may have different configurations[15] as

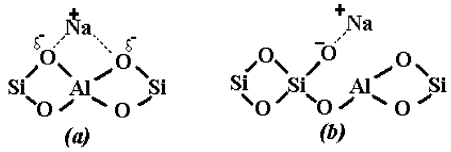

It is known that defects[15,16] like creation of mesopores and lattice faults are incorporated in the MOR structure at any of the following stages: synthesis, modification, and calcination at high temperature (773 K). So, it is reasonable to presume that some sodium ions may be located in these defects. Therefore, the three uptakes probably originated from sodium ions that are either in defects of MOR or in different configurations as (a) and (b) in the channel. The chemisorption and desorption of nitrogen in replacement experiments carried out on Li, K, Cs, Mg, Ca, and Ba samples of MOR are not prominent, probably due to the less chemisorptive nature of nitrogen on these cations.

The features found in the NaM profile can be demonstrated through a model (Figure 5). In this figure, the channel (vertical tube) and side pocket (horizontal tube) of MOR are shown with three sodium ions (depicted as closed circles) in the channels with one at the intersection and one in the side pocket. In the stream of nitrogen at <173 K, gaseous nitrogen (cross lines) filled the channels and side pockets of calcined NaM sample in addition to a portion of nitrogen condensed (dotted portions) around sodium ions. When 10% H_2/N_2 gas is turned on at 173 K, the prefilled nitrogen in channels (R_{rc}) and the nitrogen condensed (R_{hc}) around the sodium ions are rapidly replaced

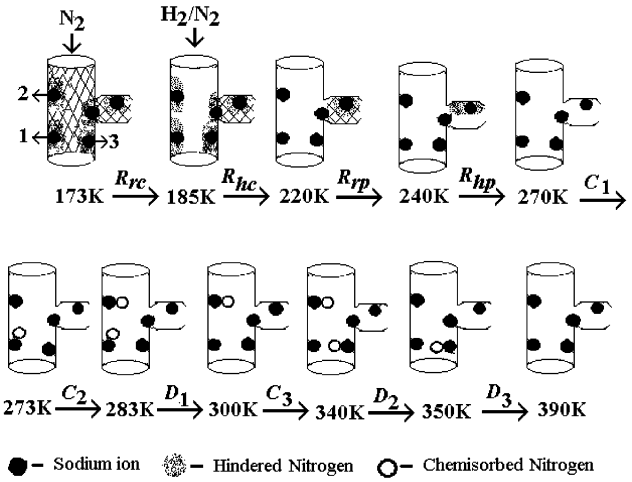

Figure 5. Model figure showing the nitrogen replacements by hydrogen in the channels and side pockets of NaM.

(hollow columns) by hydrogen at ~185 and ~220 K, respectively. Because of the small dimension, similar replacement reactions in the side pockets (R_{rp} and R_{hp}) are delayed in the model to high temperatures (240 and 270 K). When the system temperature is raised, activated nitrogen molecules chemisorb (depicted as open circles) on sodium ions. The sequence of chemisorption of nitrogen, i.e., C_1 (273 K), C_2 (283 K), and C_3 (340 K), and desorption of the chemisorbed nitrogen, i.e., D_1 (300 K), D_2 (350 K), and D_3 (390 K), from sodium−oxygen ionic pairs at the same sites is also appropriately shown in the model.

4. Conclusions

The progressive replacement of nitrogen filled in the pores of NaMOR by hydrogen has been studied by a specially designed low-temperature-programmed routine (LTR). The following consecutive phenomena have been distinguished in the routine.

1. The rapid replacement of gaseous nitrogen in the channel (185 K) and in the side pocket (240 K).

2. The hindered replacement of nitrogen condensed around sodium ions in the channel (220 K) and in the side pocket (270 K).

3. The activated chemisorption of nitrogen on the Na^+O^- pair located at three kinds of sites in MOR at $T \sim 273$ (channels), 283 (intersection), and 340 K (side pocket).

4. The desorption of chemisorbed nitrogen from these sodium−oxygen ionic pairs at 300, 350, and 390 K in NaMOR.

Notably, the replacement of nitrogen in LTR can help in resolving the complex diffusion phenomena of gases through micropores. In this temperature-programmed study, it is demonstrated that the structural dimension of micropores in zeolite and the interaction of flow gases with cation significantly affect the replacement of nitrogen in MOR pores.

Acknowledgment. We thank National Science Council for the financial assistance and one of the authors, S.Y, also thanks for the postdoctoral fellowship.

References and Notes

(1) Karger, J.; Ruthven, D. M. *Diffusion in zeolites and other microporous materials*; Wiley: New York, 1992.

(2) Nishiyama, N.; Ueyama, K.; Matsukata, M. *AIChE J.* **1997**, *43*, 2724.

(3) Shiokawa, K.; Ito, M.; Itabashi, K. *Zeolites* **1989**, *9*, 170.

(4) Stockmeyer, R. *Zeolites* **1992**, *12*, 251.

(5) Chou, C. W.; Chu, S. J.; Chiang, H. J.; Huang, C. Y.; Lee, C. J.; Sheen, S. R.; Perng, T. P.; Yeh, C. T. *J. Phys. Chem. B* **2001**, *105*, 9113.

(6) Tsapatsis, M.; Lovallo, M.; Okubo, T.; Davis, M. E.; Sadakata, M. *Chem. Mater.* **1995**, *7*, 1734.

(7) Meier, W. M.; Olson, D. H.; Baerlocher, Ch. Atlas of Zeolite Structure Types. *Zeolites* **1996**, *17*, 152.

(8) Jirka, I.; Plsek, J.; Kotrla, J. *J. Catal.* **2001**, *200*, 345.

(9) Devatour, S.; Vanderschueren, J.; Giuntini, J. C.; Henn, F.; Zanchetta, J. V.; Ginoux, J. L. *J. Phys. Chem. B* **1998**, *102*, 3749.

(10) Mortier, W. J. *Compilation of Extraframework Sites in Zeolites*; Butterworth: Guildford, 1982.

(11) Tyburce, B.; Kappenstein, C.; Cartraud, P.; Garnier, E. *J. Chem. Soc., Faraday Trans.* **1991**, *87* (17), 2849.

(12) Coughlan, B.; Carrol, W. M.; McCann, W. A. *J. Chem. Soc., Faraday Trans.* **1977**, *73*, 1612.

(13) Devautour, S.; Abdoulaye, A.; Giuntini, J. C.; Henn, F. *J. Phys. Chem. B* **2001**, *105*, 9297.

(14) Bhatia, S. *Zeolite Catalysis: Principles and Applications*; CRC Press: Boca Raton, FL, 1990; p 38.

(15) Moreau, F.; Bernard, S.; Gnep, N. S.; Lacombe, S.; Merlen, E.; Guisnet, M. *J. Catal.* **2001**, *202*, 402.

(16) Moreau, F.; Ayrault, P.; Gnep, N. S.; Lacombe, S.; Merlen, E.; Guisnet, M. *Micropor. Mesopor. Mater.* **2002**, *51*, 211.